

Transferred hyperfine interactions for trapped-hole centers in tetragonal GeO_2 †

M. Stapelbroek,* O. R. Gilliam, and R. H. Bartram

Department of Physics and Institute of Materials Science, University of Connecticut, Storrs, Connecticut 06268

(Received 28 January 1977)

γ -ray, x-ray, or uv irradiation at 77 K of single crystals of tetragonal GeO_2 containing substitutional Ga^{3+} impurity cations generates holelike centers analogous to the $[\text{Al}]^0$ centers reported previously in Al-doped crystals. The measured $[\text{Ga}]^0$ -center spin-Hamiltonian parameters are: $g_x = 2.0249 \pm 0.0003$, $g_y = 2.0132 \pm 0.0003$, $g_z = 2.0039 \pm 0.0003$; $|{}^{69}\text{A}_x| = 9.13 \pm 0.05$, $|{}^{69}\text{A}_y| = 10.27 \pm 0.05$, and $|{}^{69}\text{A}_z| = 9.62 \pm 0.05$. These \vec{A} components, in units of 10^{-4} cm^{-1} , are given for the ${}^{69}\text{Ga}$ isotope; hyperfine components for ${}^{71}\text{Ga}$ are larger by the ratio of the nuclear moments. From symmetry, the only contribution to the isotropic part of the hyperfine interaction for both $[\text{Al}]^0$ and $[\text{Ga}]^0$ centers arises from exchange core polarization. Detailed analysis, which includes calculation of the anisotropic part of the hyperfine interaction using free-ion wave functions for Al^{3+} , Ga^{3+} , and O^- , yields the signs of the hyperfine components, the internuclear distance between the impurity cation and the O^- ion, and verifies the ionic nature of the centers. A two-step mechanism is proposed for the positive exchange core polarization occurring in the $[\text{Ga}]^0$ center.

I. INTRODUCTION

Trapped-hole centers in oxide materials have received considerable experimental and theoretical attention for many years.¹ The electron-spin-resonance (ESR) spectra of many of these centers can be explained in terms of a model consisting of a hole trapped on an oxygen anion (i.e., an O^- ion) adjacent to a charge-deficient cation site. We have recently reported that such a center associated with trivalent Al impurities is observed following uv, x-ray, or γ -ray irradiation at 77 K in single crystals of tetragonal (rutile-structure) GeO_2 .² In Ref. 2, an *ab initio* point-ion crystal-field calculation was employed to support the model deduced from the ESR spectra. By analogy with similar centers observed in the alkaline-earth oxides,³ this Al-related trapped-hole center was labeled the $[\text{Al}]^0$ center. Brief reports have also been given on the analogous $[\text{Ga}]^0$ and $[\text{Y}]^0$ centers in tetragonal GeO_2 .^{4,5} Recently, trapped-hole centers associated with substitutional Al and Ga impurities in the isomorphous material SnO_2 have been reported^{6,7}; and in the anatase form of TiO_2 , an Al-related trapped-hole center has also been observed.⁸

The spin-Hamiltonian parameters for the $[\text{Ga}]^0$ center are reported in Sec. II and the remainder of this paper is devoted to an analysis of the hyperfine interaction observed for the $[\text{Al}]^0$ and $[\text{Ga}]^0$ centers in tetragonal GeO_2 . Section III describes a calculation of the anisotropic part of the transferred hyperfine interaction for these centers using free-ion wave functions for Al^{3+} , Ga^{3+} , and O^- , including overlap and covalency effects. In Sec. IV, the results of these calculations are compared to experiment, the signs of

the hyperfine parameters are inferred, and a possible mechanism for the difference in the sign of the isotropic hyperfine interaction for the $[\text{Al}]^0$ and $[\text{Ga}]^0$ centers is suggested. Comparison between these centers in tetragonal GeO_2 and the Al- and Ga-related trapped-hole centers in SnO_2 and TiO_2 (anatase) is also made in Sec. IV.

II. EXPERIMENTAL RESULTS FOR THE $[\text{Ga}]^0$ CENTER

The experimental procedure and analysis used to obtain ESR parameters for the $[\text{Ga}]^0$ center are similar to those described in Ref. 2 for the $[\text{Al}]^0$ center. The ESR spectrum for $\vec{H} \parallel [001]$ is shown in Fig. 1. For this orientation, two four-line hyperfine patterns are observed corresponding to the interaction of the unpaired spins with ${}^{69}\text{Ga}$ (60.2% naturally abundant, $I = \frac{3}{2}$) and ${}^{71}\text{Ga}$ (39.8% naturally abundant, $I = \frac{3}{2}$) nuclei. The ratio of in-

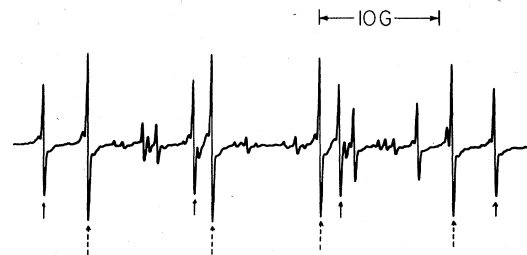


FIG. 1. ESR spectrum for the $[\text{Ga}]^0$ center with $\vec{H} \parallel [001]$. The dotted arrows indicate the "allowed" hyperfine transitions for those centers with a ${}^{69}\text{Ga}$ nucleus, while the solid arrows indicate these transitions for the centers with a ${}^{71}\text{Ga}$ nucleus. "Forbidden" hyperfine transitions can be seen in between the allowed transitions. The spectrum was recorded at 92 K and 9.2 GHz.

tensities for the two patterns is in agreement with the ratio of natural abundances, and the ratio of the splittings between the lines is in agreement with the ratio of the nuclear moments. In addition, several "forbidden" transitions are evident between the main hyperfine lines in Fig. 1. These transitions arise through the combined effect of the nuclear Zeeman interaction and the quadrupole interaction and will be analyzed in detail in a subsequent publication.⁹

The angular variation of the "allowed" hyperfine lines, shown in Fig. 2 for the ^{71}Ga isotope, reveals that there are two magnetically inequivalent sites for $\bar{\text{H}}$ in the (001) plane and three magnetically inequivalent sites for $\bar{\text{H}}$ in the (110) plane, similar to what is observed for the $[\text{Al}]^0$ center. The crystal structure for tetragonal GeO_2 is shown in Fig. 3, which illustrates inequivalent anion sites represented by (\bar{a}) and (\bar{b}) . By analogy with the $[\text{Al}]^0$ center,² the model proposed for the $[\text{Ga}]^0$ center is a hole trapped in a $2p_z$ orbital of a (\bar{b}) oxygen anion adjacent to a substitutional Ga^{3+} impurity ion (see Figs. 4 and 5). The point symmetry at the O^- lattice site is monoclinic (C_s) and therefore \bar{g} and \bar{A} have only one common principal axis (the z axis). The principal axis systems for the \bar{g} and \bar{A} tensors are defined in Fig. 4. A least-squares fit of Eq. (2) in Ref. 2 to the observed angular variation yielded the ESR parameters and the angles α and β given in Table I.

An isochronal pulse anneal was performed for both the $[\text{Al}]^0$ and $[\text{Ga}]^0$ centers. The intensity of

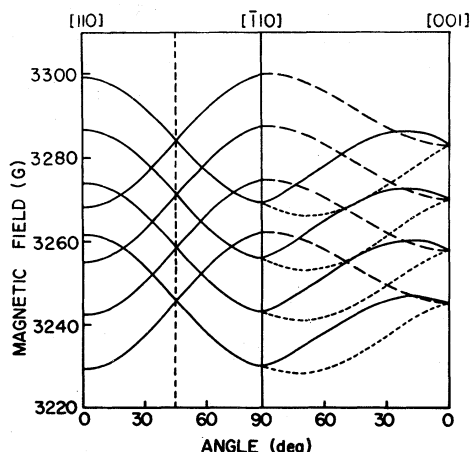


FIG. 2. Angular variation of the allowed hyperfine lines for the ^{71}Ga center with rotation of $\bar{\text{H}}$ in the (001) and (110) planes, corresponding to the left- and right-hand sides of the figure, respectively. Two four-line hyperfine patterns are observed in the (001) plane, and three are observed in the (110) plane, resulting from magnetically inequivalent sites. The angular variation for the ^{69}Ga center is similar.

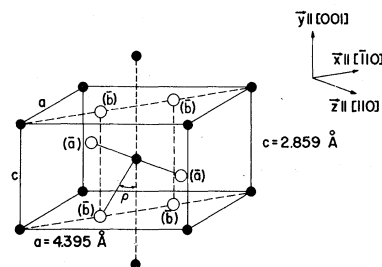


FIG. 3. Unit cell of tetragonal GeO_2 with the addition of two neighboring cations along the [001] direction. There are two inequivalent cation sites (dark circles) related by a 90° rotation about the c axis. The (\bar{a}) anions are at a slightly greater distance (1.902 \AA) from the central cation than the (\bar{b}) anions (1.872 \AA). The $\text{Ge}-\text{O}(\bar{b})$ bond direction makes an angle $\rho = 40.1^\circ$ with the c axis.

the ESR signal was first measured at 92 K without warmup after x irradiation at 77 K. The temperature was then raised in steps of 10 K and the sample was annealed for 5 min at each temperature. In between each step the temperature was lowered to 92 K and the intensity of the remaining ESR signal was recorded. The results are plotted in Fig. 6. The excellent coincidence of the experimental points for the $[\text{Al}]^0$ and $[\text{Ga}]^0$ centers suggests that the thermal decay of these centers is caused by the release into the conduction band of electrons that were trapped at an unidentified electron trap in the crystal (see note added in proof). Some difference in the thermal annealing behavior would be expected between the two centers if the annealing mechanism involved the release of the trapped hole into the valence band.

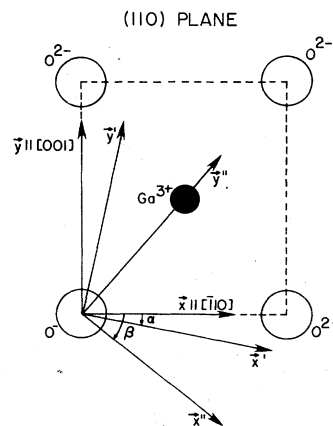


FIG. 4. Principal axes for the \bar{g} and \bar{A} tensors of the spin Hamiltonian which are represented by single- and double-primed axes, respectively. Values of α and β are listed in Table I.

III. ANISOTROPIC HYPERFINE INTERACTION

The anisotropic part of the hyperfine interaction arises from the magnetic dipole-dipole interaction between the paramagnetic electron and the magnetic moment of the nucleus. This interaction can be written in the form¹⁰

$$\mathcal{H}_{\text{dipolar}} = \vec{S} \cdot \vec{T} \cdot \vec{I}, \quad (1)$$

where

$$\vec{T} = (-g\mu_B g_N \mu_N) \begin{bmatrix} \left\langle \frac{\gamma^2 - 3x^2}{r^5} \right\rangle & -\left\langle \frac{3xy}{r^5} \right\rangle & -\left\langle \frac{3xz}{r^5} \right\rangle \\ -\left\langle \frac{3xy}{r^5} \right\rangle & \left\langle \frac{\gamma^2 - 3y^2}{r^5} \right\rangle & -\left\langle \frac{3yz}{r^5} \right\rangle \\ -\left\langle \frac{3xz}{r^5} \right\rangle & -\left\langle \frac{3yz}{r^5} \right\rangle & \left\langle \frac{\gamma^2 - 3z^2}{r^5} \right\rangle \end{bmatrix}. \quad (2)$$

In Ref. 2, it was shown that the hole was trapped in the $2p_z$ orbital of the O^- ion, leaving an electron with unpaired spin in this orbital, and that the symmetry at the defect site did not allow an admixture of $2p_x$, $2p_y$, or $2s$ orbitals with the $2p_z$ orbital. The crystal-field splitting of the energy levels was calculated using a completely ionic model and free-ion wave functions for the O^- ion. In order to calculate the hyperfine interaction, however, care must be taken to orthogonalize the wave function of the unpaired electron to the core orbitals of the Al^{3+} or Ga^{3+} ion (overlap effects) and even small amounts of covalency must be considered since covalency will appreciably affect the hyperfine interaction. (The coordinate system used in the remainder of this section is the double-primed system shown in Fig. 4, however, for simplicity in notation the double primes are omitted.)

To include the overlap and covalency effects, the wave function of the unpaired electron can be

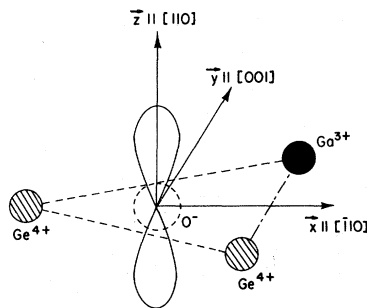


FIG. 5. Nearest-neighbor environment for the $[Ga]^0$ center in tetragonal GeO_2 . The hole is trapped in a p_z orbital of the O^- ion.

TABLE I. Experimentally determined spin-Hamiltonian parameters for the $[Ga]^0$ center in tetragonal GeO_2 . The \bar{A} tensor components are in units of 10^{-4} cm^{-1} . The angles α and β are defined in Fig. 4.

g_x'	2.0249 ± 0.0003	
g_y'	2.0132 ± 0.0003	
g_z'	2.0039 ± 0.0003	
α	$19.4^\circ \pm 0.5^\circ$	
	$[^{71}Ga]^0$	$[^{69}Ga]^0$
$ A_{xx''} $	11.49 ± 0.05	9.13 ± 0.05
$ A_{yy''} $	12.89 ± 0.05	10.27 ± 0.05
$ A_{zz''} $	11.85 ± 0.05	9.62 ± 0.05
β	$36^\circ \pm 2^\circ$	

written¹¹

$$|\psi\rangle = N^{-1/2} \left(|2p_z^0\rangle - \sum_i \lambda_i |\phi_i\rangle \right), \quad (3)$$

where

$$\lambda_i = \gamma_i + S_i, \quad (4a)$$

$$S_i = \langle \phi_i | 2p_z^0 \rangle, \quad (4b)$$

and

$$N = 1 - \sum_i (2\lambda_i S_i - \lambda_i^2). \quad (4c)$$

In these equations, $|2p_z^0\rangle$ is the $2p_z$ orbital of the O^- ion, the $|\phi_i\rangle$ are the Al^{3+} (Ga^{3+}) core orbitals, γ_i is a parameter that describes the covalency ($\gamma_i = 0$ corresponds to the completely ionic case), and S_i is an overlap integral.

Symmetry considerations immediately reduce the number of core orbitals that can be admixed into the wave function. Both the O^- ion and the impurity ion are located on the (110) mirror plane and the unpaired electron is in an orbital that is odd under reflection through the mirror plane. The only core orbitals that can be admixed into the wave

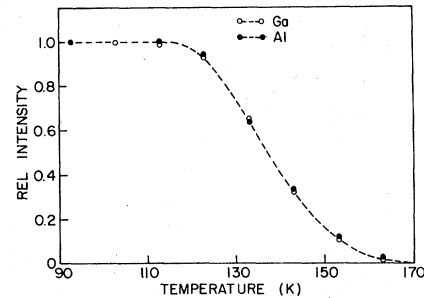


FIG. 6. Isochronal pulse anneal for the $[Al]^0$ and $[Ga]^0$ centers in tetragonal GeO_2 . The samples were annealed for 5 min at each temperature and the temperature was increased in steps of 10 K. The samples were returned to 92 K for the intensity measurement following each anneal.

function must also be odd. The only core orbital meeting this requirement for Al^{3+} (ground-state configuration $1s^2 2s^2 2p^6$) is the $2p_z$ orbital, while for Ga^{3+} (ground-state configuration $1s^2 2s^2 2p^6 3s^2 3p^6 3d^{10}$) only the $2p_z$, $3p_{zx}$, and $3d_{yz}$ core orbitals meet this requirement. However, the overlap integral $S(2p_z^O, 3d_{zx}^{\text{Ga}}) = \langle 2p_z^O | 3d_{zx}^{\text{Ga}} \rangle$ vanishes and the covalency with this orbital is expected to be negligible compared to the covalency with the $3d_{yz}$ orbital. For the $[\text{Al}]^0$ center, then, the wave function of the unpaired electron can be written

$$|\psi^{\text{Al}}\rangle = N_{\text{Al}}^{-1/2} (|2p_z^O\rangle - \lambda_{2p}^{\text{Al}} |2p_z^{\text{Al}}\rangle), \quad (5)$$

and for the $[\text{Ga}]^0$ center as

$$|\psi^{\text{Ga}}\rangle = N_{\text{Ga}}^{-1/2} (|2p_z^O\rangle - \lambda_{2p}^{\text{Ga}} |2p_z^{\text{Ga}}\rangle - \lambda_{3p}^{\text{Ga}} |3p_z^{\text{Ga}}\rangle - \lambda_{3d}^{\text{Ga}} |3d_{yz}^{\text{Ga}}\rangle). \quad (6)$$

The anisotropic hyperfine tensor can now be expressed as

$$\begin{aligned} \bar{\mathbf{T}}_{\text{Al}} = N_{\text{Al}}^{-1} \{ & \bar{\mathbf{T}}(2p_z^O, 2p_z^O) - 2\lambda_{2p}^{\text{Al}} \bar{\mathbf{T}}(2p_z^O, 2p_z^{\text{Al}}) \\ & + (\lambda_{2p}^{\text{Al}})^2 \bar{\mathbf{T}}(2p_z^{\text{Al}}, 2p_z^{\text{Al}}) \} \end{aligned} \quad (7)$$

for the $[\text{Al}]^0$ center, and as

$$\begin{aligned} \bar{\mathbf{T}}_{\text{Ga}} = N_{\text{Ga}}^{-1} \{ & \bar{\mathbf{T}}(2p_z^O, 2p_z^O) - 2\lambda_{2p}^{\text{Ga}} \bar{\mathbf{T}}(2p_z^O, 2p_z^{\text{Ga}}) \\ & - 2\lambda_{3p}^{\text{Ga}} \bar{\mathbf{T}}(2p_z^O, 3p_z^{\text{Ga}}) \\ & - 2\lambda_{3d}^{\text{Ga}} \bar{\mathbf{T}}(2p_z^O, 3d_{yz}^{\text{Ga}}) + (\lambda_{2p}^{\text{Ga}})^2 \bar{\mathbf{T}}(2p_z^{\text{Ga}}, 2p_z^{\text{Ga}}) \\ & + (\lambda_{3p}^{\text{Ga}})^2 \bar{\mathbf{T}}(3p_z^{\text{Ga}}, 3p_z^{\text{Ga}}) + (\lambda_{3d}^{\text{Ga}})^2 \bar{\mathbf{T}}(3d_{yz}^{\text{Ga}}, 3d_{yz}^{\text{Ga}}) \\ & + \lambda_{2p}^{\text{Ga}} \lambda_{3p}^{\text{Ga}} \bar{\mathbf{T}}(2p_z^{\text{Ga}}, 3p_z^{\text{Ga}}) \}, \end{aligned} \quad (8)$$

for the $[\text{Ga}]^0$ center. The terms $\bar{\mathbf{T}}(2p_z^{\text{Ga}}, 3d_{yz}^{\text{Ga}})$ and $\bar{\mathbf{T}}(3p_z^{\text{Ga}}, 3d_{yz}^{\text{Ga}})$ are not included in Eq. (8); they vanish because the angular parts of these integrals vanish. In Eqs. (7) and (8), the notation $\bar{\mathbf{T}}(\phi_1, \phi_2)$ means that the matrix elements are evaluated between orbitals ϕ_1 and ϕ_2 .

The matrix elements appearing in Eqs. (7) and (8) were evaluated using Clementi's¹² analytic free-ion wave functions for the O^- ion and numerical $X\alpha$ free-ion wave functions for the Al^{3+} and Ga^{3+} ions. The $X\alpha$ wave functions were computed using the program written by Herman and Skillman¹³ modified to use the correct value of α as recommended by Slater.¹⁴ The two-center integrals appearing in Eqs. (7) and (8) were reduced to a form convenient for numerical integration by the method outlined in Ref. 15. Anisotropic hyperfine tensor components were evaluated for distances between the ions ranging from 2 to 5 a.u. The results for the completely ionic case (i.e., $\lambda_i = S_i$) are plotted in Figs. 7 and 8 for the $[\text{Al}]^0$ and $[\text{Ga}]^0$ centers, respectively. Figure 7 shows that for an internuclear distance D of 5 a.u., the calculated $\bar{\mathbf{T}}$ tensor for the $[\text{Al}]^0$ is approximately axial, in-

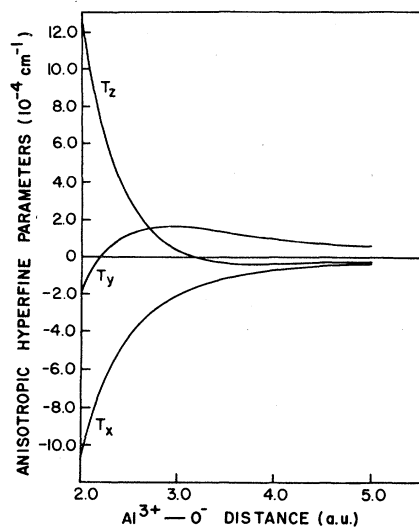


FIG. 7. Calculated anisotropic hyperfine interaction as a function of $\text{Al}^{3+}-\text{O}^-$ internuclear distance. This figure shows the completely ionic case where $\lambda = S(2p_z^O, 2p_z^{\text{Al}})$.

dicating that a point-dipole model would adequately describe the anisotropic hyperfine interaction for this center. However, an appreciable deviation from axial symmetry is predicted for the $[\text{Ga}]^0$ center at this distance, as depicted in Fig. 8. At smaller internuclear distances the effect of overlap with the outer p_x core orbital becomes dominant.

IV. DISCUSSION

While the magnitudes of the hyperfine parameters for the $[\text{Al}]^0$ and $[\text{Ga}]^0$ centers have been

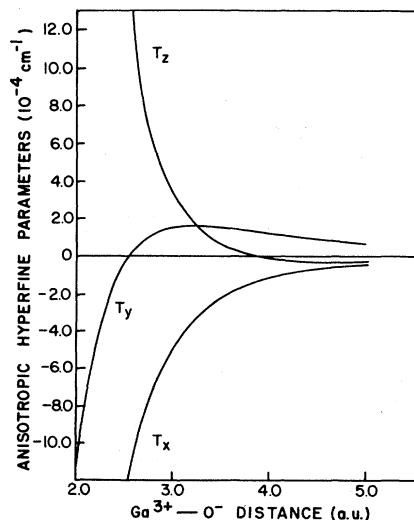


FIG. 8. Calculated anisotropic hyperfine interaction as a function of $\text{Ga}^{3+}-\text{O}^-$ internuclear distance. This figure shows the completely ionic case.

determined from the ESR data, no direct experimental information has been obtained on the signs of these parameters. The signs must be inferred either from theory or from a comparison with similar centers in other materials, or from both. Of the eight possible sign combinations for the hyperfine tensor principal values, only two for each center are consistent with the theoretical calculation of Sec. III, even when covalency effects are included.¹⁵ In view of the similarities between the two centers, however, the only consistent choice that can be made gives the $[\text{Al}]^0$ center hyperfine parameters as all negative while the $[\text{Ga}]^0$ center hyperfine parameters are all positive.¹⁵ In addition, the best agreement of calculated hyperfine parameters with experiment is obtained with no covalency introduced and an internuclear distance D about 40% greater than the undistorted lattice distance of 3.6 a.u. These results tend to support the assumptions made in Ref. 2 of negligible covalency and of the reduction in the strength of the crystal field due to lattice distortion.

Further support for these choices of the signs of the hyperfine interaction is obtained from comparison with similar centers in other oxide materials. Schirmer¹⁶ has studied the $[\text{Li}]^0$ center in ZnO and BeO and also has inferred that the Li^+-O^- bond length increases by about 40% over the normal lattice distance in these oxides. The $[\text{Li}]^0$ and $[\text{Na}]^0$ centers in MgO, CaO, and SrO have been well characterized by electron-nuclear-double-resonance (ENDOR) techniques³ and the increased lattice distance is observed for the $[\text{Li}]^0$ center in all three hosts and for the $[\text{Na}]^0$ center in SrO, although for $\text{CaO}:[\text{Na}]^0$ the distance was essentially unchanged and for $\text{MgO}:[\text{Na}]^0$ a decrease in the distance was noted. This decrease was discussed in terms of the disparity in ionic radii between the Na^+ and Mg^{2+} ions. Similar increases in internuclear distance are observed for the $[\text{Al}]^0$ and $[\text{Ga}]^0$ centers in SnO_2 .⁶ For tetragonal GeO_2 and SnO_2 , however, the outward relaxation may be helped by the spaciousness of the rutile lattice.¹⁷

Because the trivalent impurity ion constitutes an effective negative charge in the lattice and the trapped hole constitutes an effective positive charge, the relaxation of these two ions away from each other may seem surprising at first glance. It is precisely the attraction between these effective charges that causes the hole to localize adjacent to the trivalent impurity lattice site. Once localized, however, a more microscopic picture is appropriate. Using the purely ionic picture that has been established for these centers, the reason for the outward relaxation of these ions is simply that the electrostatic attraction between a trivalent cation and a monoval-

ent anion is less than the attraction between a quadrivalent cation and a divalent anion. Therefore, for the $[\text{Al}]^0$ and $[\text{Ga}]^0$ centers, an outward relaxation is expected.

The existence of a nonzero isotropic hyperfine interaction for both the $[\text{Al}]^0$ and $[\text{Ga}]^0$ centers implies the presence of a nonzero unpaired-spin density at the respective magnetic nucleus. Because the impurity ion's magnetic nucleus is located on a nodal plane of the $2p_z$ orbital of the O^- ion, the wave function of the unpaired spin must be identically zero at the magnetic nucleus. The unpaired-spin density must therefore arise from exchange core polarization. Exchange core polarization has been proposed as the mechanism responsible for the negative transferred hyperfine interactions observed for the V_k center in LiF ,^{18,19} and also for the $[\text{Li}]^0$ center in ZnO, BeO,¹⁶ MgO, CaO, and SrO,³ and for the $[\text{Na}]^0$ center in MgO, CaO, and SrO.³

The exchange core-polarization contribution to the Fermi-contact hyperfine interaction can be described by²⁰

$$a_0 = \frac{2}{3}g\mu_B g_N \mu_N \chi, \quad (9)$$

where χ represents the difference in the density of spin-up (+) and spin-down(-) electrons at the nucleus, that is,

$$\chi = \frac{4\pi}{2S} \sum_i \{ |\phi_i^+(0)|^2 - |\phi_i^-(0)|^2 \}. \quad (10)$$

Here, the sum ranges over the core s orbitals of the Al or Ga ion, $S = \frac{1}{2}$, and $|\phi_i^{\pm}(0)|^2$ means the density at the nucleus for electrons with spin parallel to that of the paramagnetic electron. Values of the core-polarization parameter χ calculated from experiment for the $[\text{Al}]^0$ and $[\text{Ga}]^0$ centers are given in Table II.

The sign of the core-polarization parameter χ has been found to vary for transferred hyperfine interactions in similar centers. Schirmer²¹ has attributed this change in sign to a variation in the size of the overlap between the unpaired spin wave function and the ligand core s orbitals. The results of the present study indicate that another mechanism can also yield positive exchange core polarization since, for the $[\text{Ga}]^0$ center, overlap of the unpaired spin with the Ga^{3+} ion-core s orbitals vanishes by symmetry. Polarization outward of the outer shells of the Ga^{3+} ion by the unpaired electron may lead to a reduced exchange interaction between the (+) spin outer-shell electrons and (+) spin inner-shell s electrons. The reduced attractive interaction between the outer-shell electrons and the inner-shell s orbitals may result in an inward relaxation of the (+) spin inner-shell s electrons and a net positive spin density

TABLE II. Results of the hyperfine analysis for the $[\text{Al}]^0$ and $[\text{Ga}]^0$ centers in tetragonal GeO_2 . Signs of the components of \bar{A} are inferred from the analysis. Hyperfine parameters are given in units of 10^{-4} cm^{-1} ; core polarization χ and internuclear distance D are given in a.u. Calculated \bar{T} components and their appropriate signs are given for the best agreement between experiment and theory, with D as an adjustable parameter.

Parameter	$[\text{Al}]^0$	$[\text{Ga}]^0$
A_x	-4.50	+11.49
A_y	-3.57	+12.89
A_z	-4.51	+11.85
T_x	-0.31(-0.35) ^a	-0.59(-0.53)
T_y	+0.62(+0.63)	+0.81(+0.81)
T_z	-0.32(-0.27)	-0.23(-0.28)
a_0	-4.19	+12.08
χ	-0.136	+0.334
D	5.0	4.9

^a Values in parentheses are theoretical values calculated for the given internuclear distance D .

at the Ga^{3+} nucleus. A two-step mechanism such as this may explain the observed positive core polarization for the $[\text{Ga}]^0$ center in tetragonal GeO_2 .

Several significant differences are apparent in comparing the $[\text{Al}]^0$ and $[\text{Ga}]^0$ centers in SnO_2 (Ref. 6) with those observed in tetragonal GeO_2 . For SnO_2 : $[\text{Al}]^0$, at low temperatures, the trapped hole is localized on an (\bar{a}) -type anion⁶; and above 115 K motional effects, attributed to the hole hopping between the two equivalent (\bar{a}) anions, begin to average the ESR spectrum.⁶ Furthermore, from the directions of the principal axes of the A tensor, it was inferred that, even at low temperatures, the trapped hole tunnels between two closer (\bar{b}) anions in the SnO_2 : $[\text{Ga}]^0$ center.⁶ These results are not observed for the trapped-hole centers in tetragonal GeO_2 (that is, the hopping or tunneling rate is significantly less than the microwave frequency). Furthermore, observation of trapped-hole centers in tetragonal GeO_2 at higher temperatures, where motional effects could become evident, is difficult, because the centers begin to anneal at about 120 K.

A radiation-induced trapped-hole center associated with a substitutional Al^{3+} impurity cation in single crystals of the anatase phase of TiO_2 bears a striking resemblance to the $[\text{Al}]^0$ center in tetragonal GeO_2 .⁸ This similarity arises because, in spite of the different crystal structures, there are four magnetically inequivalent O^- sites in each

material, these inequivalent sites are oriented approximately the same with respect to the crystal axes in both materials, and the point symmetry at the O^- site is $C_{2v}(m)$ in both materials. The only significant difference in the two centers is that the Al^{3+} - O^- bond directions are 40° and 80° from the c axis in tetragonal GeO_2 and anatase, respectively. This difference in bond direction is obtained from the change in the orientation of the hyperfine tensor principal axes in the two cases.^{2,8}

V. SUMMARY

Two impurity-related trapped-hole centers designated the $[\text{Al}]^0$ and $[\text{Ga}]^0$ centers, occurring in Al- and Ga-doped single crystals of tetragonal GeO_2 , respectively, following ionizing irradiation at liquid-nitrogen temperatures, have been observed by ESR. Detailed analysis of the ESR data combined with an *ab initio* point-ion crystal-field calculation² supports a model in which a hole is trapped in a $2p_z$ (π -type) orbital on one of the four nearest-neighbor (\bar{b}) anions adjacent to a substitutional Al^{3+} or Ga^{3+} impurity ion. A theoretical analysis of the anisotropic hyperfine interaction for these two centers shows that a completely ionic model is an appropriate description for these centers and supports the contention that the crystal field at the O^- site is reduced by distortion. The analysis of the hyperfine structure for these two centers provides the signs of the hyperfine tensor components and thereby the sign and magnitude of the core polarization for each center. The positive sign of the core polarization for the $[\text{Ga}]^0$ center has been tentatively explained by a two-step mechanism of core polarization. Thus the ESR data and the theoretical analysis have resulted in a fairly complete description of the electronic structure of these two trapped-hole centers.

Note added in proof. Subsequent measurements in this laboratory on trapped-hole centers associated with Mg impurity cations do not appear to support this argument.

ACKNOWLEDGMENTS

We wish to thank T. J. Welsh for his help on experimental measurements for the $[\text{Ga}]^0$ center and Dr. E. Kostiner for assistance in the preparation of the single crystals used in this study. The computational portions of this investigation were performed at the University of Connecticut Computer Center.

- *Present address: Code 6440, Naval Research Laboratory, Washington, D. C. 20375.
- †Supported by the U. S. Army Research Office, Durham, Grant No. DAHCO4-75-G-0128 and by the University of Connecticut Research Foundation.
- ¹A. E. Hughes and B. Henderson, in *Point Defects in Solids*, edited by J. H. Crawford, Jr. and L. M. Slifkin (Plenum, New York, 1972), Vol. 1, Chap. 7.
- ²M. Stapelbroek, R. H. Bartram, O. R. Gilliam, and D. P. Madacsi, *Phys. Rev. B* **13**, 1960 (1976).
- ³M. M. Abraham, W. P. Unruh, and Y. Chen, *Phys. Rev. B* **10**, 3540 (1974).
- ⁴T. J. Welsh, M. Stapelbroek, and O. R. Gilliam, *Bull. Am. Phys. Soc.* **20**, 808 (1975).
- ⁵R. B. Bossoli, M. Stapelbroek, and O. R. Gilliam, *Bull. Am. Phys. Soc.* **21**, 346 (1976).
- ⁶D. Zwingel, *Phys. Status Solidi B* **77**, 171 (1976).
- ⁷E. Mollwo and D. Zwingel, *J. Lumin.* **12/13**, 441 (1976).
- ⁸V. S. Grunin, G. D. Davtyan, V. A. Ioffe, and I. B. Patrino, *Phys. Status Solidi B* **77**, 85 (1976).
- ⁹M. Stapelbroek, R. H. Bartram, and O. R. Gilliam (unpublished).
- ¹⁰J. E. Wertz and J. R. Bolton, *Electron Spin Resonance* (McGraw-Hill, New York, 1972), pp. 140-144.
- ¹¹A. Abragam and B. Bleaney, *Electron Paramagnetic Resonance of Transition Ions* (Clarendon, Oxford, England, 1970), p. 766.
- ¹²E. Clementi, *IBM J. Res. Dev. Suppl.* **9**, 2 (1965).
- ¹³F. Herman and S. Skillman, *Atomic Structure Calculations* (Prentice-Hall, Englewood Cliffs, New Jersey, 1963).
- ¹⁴J. C. Slater, *Adv. Quantum Chem.* **6**, 1 (1972).
- ¹⁵M. Stapelbroek, Ph.D. thesis (University of Connecticut, 1976) (unpublished).
- ¹⁶O. F. Schirmer, *J. Phys. Chem. Solids* **29**, 1407 (1968).
- ¹⁷F. J. Arlinghaus and W. A. Albers, Jr., *J. Phys. Chem. Solids* **32**, 1455 (1971).
- ¹⁸R. Gazzinelli and R. L. Miehler, *Phys. Rev. Lett.* **12**, 644 (1964).
- ¹⁹D. Ikenberry, A. N. Jette, and T. P. Das, *Phys. Rev. B* **1**, 2785 (1970).
- ²⁰Reference 11, pp. 697-703.
- ²¹O. F. Schirmer, *J. Phys. C* **6**, 300 (1973).